Comparison of the Hydrogen-Exchange Behavior of Reduced and Oxidized *Escherichia coli* Thioredoxin†

Mei-Fen Jeng and H. Jane Dyson*

Department of Molecular Biology, The Scripps Research Institute, La Jolla, California 92037

Received August 31, 1994; Revised Manuscript Received October 31, 1994

ABSTRACT: Hydrogen−deuterium exchange rates for the amide protons in oxidized (disulfide) and reduced (dithiol) thioredoxin have been measured using a series of $^{15}N-^{1}H$ HSQC spectra at various times after buffer exchange into 99% $^{2}H_2O$. Information on exchange rates and protection factors was obtained for both forms of thioredoxin for 68 amide protons using this method; in general, the rates obtained by this method were for amide protons of residues in the hydrogen-bonded β-sheet and α-helix secondary structure of thioredoxin. Estimates of the exchange rate for those amide protons that exchanged with rates too fast to measure by hydrogen−deuterium exchange were made by saturation-transfer measurements, which were particularly useful in defining the hydrogen exchange behavior of the active site Cys-Gly-Pro-Cys sequence and of the loops adjacent to it (residues 73−75 and 91−98). Amide proton exchange rates provide a qualitative estimate of the backbone mobility, and the differences in hydrogen exchange behavior between the two forms of thioredoxin are consistent with those observed in calculations of polypeptide chain dynamics obtained from ^{15}N relaxation measurements [Stone, M. J., *et al.* (1993) *Biochemistry 32,* 426−435]. For most of the protein, the exchange rates are close to identical in the two forms, consistent with their very close similarity in structure and backbone dynamics. Significant differences in behavior are observed in the active site sequence and in the regions of the protein that are close to this sequence in the three-dimensional structure, including portions of the β-strand and α-helical sequences immediately adjacent to the active site. In particular, the exchange rate of the Cys 35 amide proton is significantly slowed for oxidized thioredoxin compared with the reduced form. In general, the amide proton exchange rates are consistently lower for the oxidized form of thioredoxin, in accord with literature reports of lower mobility of the polypeptide backbone in the vicinity of the active site compared with the reduced protein. The rather generalized loosening of the protein structure upon reduction, indicated by the hydrogen exchange measurements, provides further evidence that the functional differences observed between the two forms of thioredoxin can most likely be ascribed to the greater flexibility of the reduced form of the protein.

Thioredoxin from *Escherichia coli* is a small, thermally stable protein containing 108 residues (M_r = 11 700), with the active site Cys_{32}-Gly-Pro-Cys_{35} forming a disulfide bond in the oxidized form (Holmgren, 1985). Oxidized thioredoxin (Trx-S_2) is usually reduced by NAPH and the flavoprotein thioredoxin reductase to a dithiol in the reduced form. Reduced thioredoxin (Trx-$(SH)_2$) is a powerful protein disulfide reductase which catalyzes dithiol−disulfide exchange reactions (Holmgren, 1985). Complete resonance assignments have been obtained for the NMR spectra of the reduced and oxidized forms in solution (Dyson *et al.,* 1989; Chandrasekhar *et al.,* 1991, 1994). The three-dimensional structure of Trx-S_2 has been solved by X-ray crystallography and refined to 1.7-Å resolution (Katti *et al.,* 1990), and the NMR solution structure of Trx-$(SH)_2$ has been calculated and refined using distance geometry and molecular dynamics (Dyson *et al.,* 1990; Jeng *et al.,* 1994). The structures of Trx-S_2 and Trx-$(SH)_2$ show a global fold containing three α-helices, one 3_{10} irregular helix, and a five-stranded twisted β-sheet.

Structural differences between Trx-$(SH)_2$ and Trx-S_2 are small and limited to the vicinity of the active site (Jeng *et al.,* 1994), yet several viral systems have an absolute requirement for Trx-$(SH)_2$ that is not solely related to the presence of active site thiols. Studies of active site mutant thioredoxins in the DNA polymerase and exonuclease activities of the phage T7 gene 5 protein (Huber *et al.,* 1986) indicate that the requirement for Trx-$(SH)_2$ rather than Trx-S_2 is at least partly due to some form of structural difference between the two forms. A comparison of backbone and tryptophan side-chain dynamics of reduced and oxidized *E. coli* thioredoxin (Stone *et al.,* 1993) shows that the difference may reside in conformations other than the ground state that are available in Trx-$(SH)_2$ but not in Trx-S_2 due to the disulfide bond. In the present work, we further characterize this difference in local structure, stability, and mobility using NMR techniques to determine amide proton hydrogen exchange.

Hydrogen exchange can provide both structural and dynamic information in a site-specific manner. Many parameters affect the intrinsic hydrogen exchange rate at a given site, including local amino acid sequence, pH, and temperature (Englander & Poulsen, 1969; Molday *et al.,* 1972; Bai *et al.,* 1993). Correction of protein exchange data for these effects has allowed the structural effects on

† Supported by Grant GM43238 from the National Institutes of Health.

* Author to whom correspondence should be addressed.

⊗ Abstract published in *Advance ACS Abstracts,* December, 1, 1994.

0006-2960/95/0434-611$09.00/0

exchange rates to be isolated, increasing the utility of these measurements for protein structural work. NMR hydrogen exchange measurements have been used extensively to characterize a number of proteins (Hughson *et al.,* 1990; Jeng & Englander, 1991; Jeng *et al.,* 1990). Apart from the intrinsic utility of the site-specific hydrogen exchange rates themselves, these measurements have become the basis for a vast new field, the study of protein folding rates using flow-quench methods (Roder, 1989). The availability of uniformly ^{15}N-labeled protein has simplified the task of data gathering for hydrogen exchange studies, since for most small proteins the ^{15}N−^{1}H HSQC spectrum is well-resolved, and can be acquired at acceptable signal/noise in a short time, allowing data points to be added rapidly in the early stages of the time course. This method has been used previously (Skelton *et al.,* 1992).

The hydrogen exchange behavior of reduced and oxidized *E. coli* thioredoxin has been studied previously (Kaminsky & Richards, 1992a), using classical methods with tritium. A difference of 3−5 amide protons observed early in proton out-exchange of the whole protein was localized to two sites in the protein, the active site loop and the first β-strand. These authors suggest that these differences can be explained by changes in the hydration of the protein as well as in the protein itself (Kaminsky & Richards, 1992a, b). The NMR hydrogen exchange methods have the advantage that the information obtained is site-specific. In this study, we utilize NMR hydrogen−deuterium exchange of uniformly ^{15}N-labeled protein under native conditions, together with saturation transfer measurements to estimate exchange rates that are too fast to measure by H−D exchange, to measure NH exchange rates for all of the backbone amide protons in both oxidized and reduced forms of *E. coli* thioredoxin.

MATERIALS AND METHODS

Sample Preparation. Uniformly ^{15}N-labeled *E. coli* thioredoxin was prepared as described previously (Chandrasekhar *et al.,* 1991). Solutions of oxidized and reduced thioredoxin (~3 mM) were prepared in 0.1 M potassium phosphate in $^{1}H_2O$ and adjusted to pH 5.7 by adding 0.1 M HCl or KOH. Hydrogen−deuterium (H−D) exchange was initiated by transferring the protein into 0.1 M potassium phosphate/$^{2}H_2O$ solution adjusted to pD 5.7 (uncorrected electrode reading). The protein solution was spun in a bench-top centrifuge using a Sephadex G-25 spin column (3-mL bed volume; 30-s centrifugation at ~400*g*). Exchange measurements were carried out under temperature-controlled conditions in the magnet at 298 K for the first 24-h period, and thereafter at intervals of days to weeks as time points were acquired to obtain data for slowly exchanging amide protons; the solution was incubated in a water bath at 298 K at other times. The range of time points was from 5 min to 723 h.

NMR Spectroscopy. ^{15}N HSQC NMR spectra were recorded at 298 K on a Bruker AMX-500 spectrometer operating in the inverse detection mode at 500.13 MHz for ^{1}H and 50.68 MHz for ^{15}N; standard pulse sequences and phase-cycling schemes were used (Bax *et al.,* 1990; Norwood *et al.,* 1990). The solvent resonance was suppressed by presaturation at low power during the recycle delay (1.2 s). All spectra were collected with the same acquisition parameters, with two transients of 2048 complex data points covering spectral widths of 6250 Hz for ω_2 and 2000 Hz for ω_1, with 128 t_1 increments. Total acquisition time was 11 min 39 s.

Fourier transformation of the data was carried out on a Sun workstation with the program FTNMR (Hare Research). Phase-shifted sine bell window functions were used in both dimensions, and the data were zero-filled to 2K in both dimensions.

Saturation-Transfer Measurements. To investigate exchange rates that are too fast to measure by the conventional H−D exchange method, the method of saturation transfer from $^{1}H_2O$ to amide protons was used (Hoffman & Forsén, 1966). The extent of amide proton exchange under these conditions was estimated by measuring and comparing peak intensities in ^{15}N HSQC spectra acquired with preirradiation of the water resonance for 3 μs, 1.0 s and 3.0 s. The residual water resonance was suppressed by high-power ^{1}H purge pulses (21.7-kHz field strength applied for approximately 0.5 and 1 ms) (Messerle *et al.,* 1989). For each of the three experiments, 32 transients were recorded for 256 increments of t_1. In order to eliminate the effects of truncated driven NOEs from C$^{\alpha}$H resonances close to the water resonance to those of amide protons, measurements were made at two different pHs (Campbell *et al.,* 1978; van de Ven *et al.,* 1988; Spera *et al.,* 1991). The two pHs, 5.7 and 6.1, were chosen to minimize the effects of several groups which titrate in the vicinity of the active site with pK_as ~ 6.7 − 7.0 (Dyson *et al., 1991*). In order that the results from the H−D exchange measurements could be compared directly with those obtained from the saturation-transfer experiments, the results at pH(apparent) 5.7 in $^{2}H_2O$ are compared with those at pH(actual) 6.1 in $^{1}H_2O$. The difference of 0.4 pH unit is applied in this case to correct for the deuterium isotope effect in the H−D exchange measurements.

Data Analysis. Hydrogen−deuterium exchange was followed by measurement of peak volumes in HSQC spectra acquired at different times after transfer of the protein to $^{2}H_2O$. The data were fitted by nonlinear least squares to a single-exponential decay and the uncertainty in the peak volumes was estimated by comparison with the amplitude of the noise of the spectrum. Uncertainties in the calculated amide proton exchange rate constants were estimated corresponding to standard deviations calculated from the covariance matrix of the nonlinear optimization routine (Skelton *et al.,* 1992).

For the saturation-transfer experiments, the exchange rates were obtained from Eq 1 (Forsén & Hoffman, 1963):

$$I(t) = I(0)[1 - [k_{ex}T_1/(1 + k_{ex}T_1)](1 - \exp(-t(1 + k_{ex}T_1))/T_1)] \quad (1)$$

where $I(t)$ is the intensity after t (=3.0) seconds of water saturation, $I(0)$ is the peak intensity with no water saturation (i.e., when t = 3 μs), T_1 is the longitudinal relaxation time of the amide proton, and k_{ex} is the amide proton exchange rate constant. An average T_1 value of 0.5 s for the amide protons in Trx-$(SH)_2$ and Trx-S_2 was estimated by inversion−recovery (Skelton *et al.,* 1992). The T_1 is short compared to the irradiation time t; eq 1 can therefore be reduced to

$$\frac{I(t)}{I(0)} = \frac{1}{(1 + k_{ex}T_1)} \quad (2)$$

and an estimate of k_{ex} can thus be made by comparison of

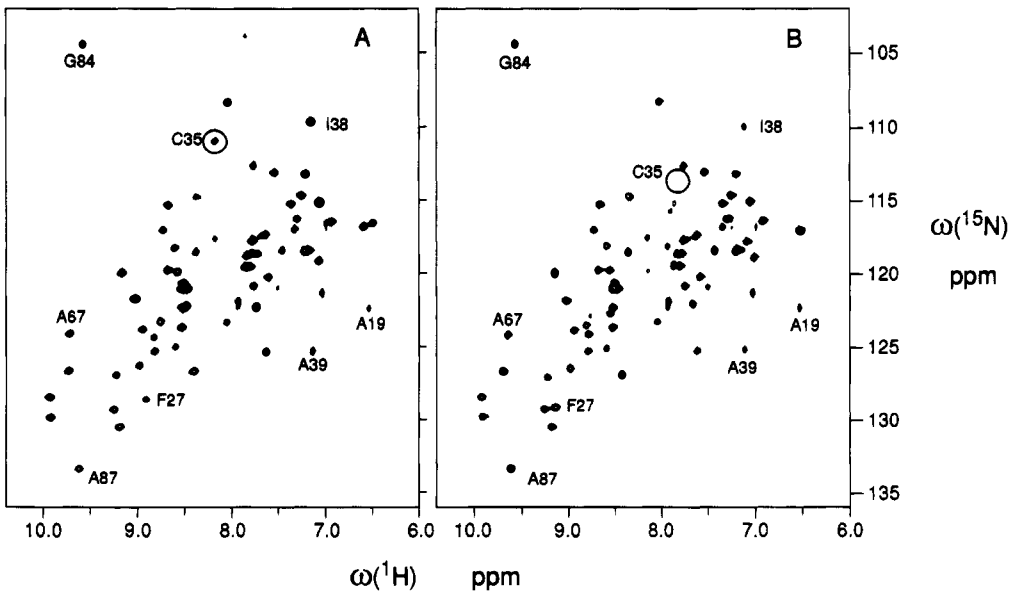

FIGURE 1: $^{15}N-^{1}H$ HSQC spectra of (A) Trx-S_2 and (B) Trx-$(SH)_2$ showing the earliest (5 min) time point after transfer of the protein into $^{2}H_2O$. Note that the cross peak for Cys 35 is present in the Trx-S_2 spectrum and absent in the Trx-$(SH)_2$ spectrum.

the intensity of peaks in the ^{15}N HSQC spectra acquired with 3 μs and 3.0 s of water saturation.

Exchange rates and protection factors were calculated as previously described (Jeng & Englander, 1991), using intrinsic rate constants calculated by the method of Englander and Poulsen (1969). The corrections for nearest-neighbor effects were made according to the data of Bai *et al.* (1993) and were calculated at pH(apparent) 5.7 for the H−D exchange results and at pH 6.1 for the saturation-transfer results, according to published methods (Connelly *et al.*, 1993).

Correction for the effect of truncated driven nuclear Overhauser enhancement from resonances close to the water resonance was made by making the saturation transfer measurements at two pHs. The actual exchange rate k_{ex}' at a given pH can be calculated according to eq 3 (Spera *et al.*, 1991):

$$k_{ex}' = (k_{ex1} - k_{ex2})/(1 - 10^{\Delta pH}) \quad (3)$$

where k_{ex1} and k_{ex2} are the exchange rates calculated at the two pH values and ΔpH is the difference between these two pHs.

RESULTS AND DISCUSSION

Measurement of Hydrogen−Deuterium Exchange Rates. A total of 30 data points were recorded for Trx-$(SH)_2$ and 26 for Trx-S_2 at different times after initial buffer exchange into $^{2}H_2O$. The extent of exchange at individual NH sites was quantified by recording HSQC spectra for each sample under identical conditions. The $^{1}H-^{15}N$ HSQC spectrum of both forms of thioredoxin is well-resolved (Chandrasekhar *et al.*, 1991). In the initial (5 min) $^{15}N-^{1}H$ HSQC spectrum there were 69 resolved $^{15}N-H$ cross peaks for Trx-S_2, and 68 for Trx-$(SH)_2$, representing about 64% of the molecule, as shown in Figure 1. A cross peak is visible for the Cys 35 amide for Trx-S_2 (Figure 1A) but not for Trx-$(SH)_2$ (Figure 1B), a strong indication that the exchange rates differ widely for this amide proton between the two forms.

All of the cross peaks were assigned according to previously published ^{1}H and ^{15}N assignments (Dyson *et al.*, 1989; Chandrasekhar *et al.*, 1991). Cross-peak volumes were measured and normalized to the average volumes of two long-lived cross peaks, Phe 81 and Leu 24. Only very few resonances could not be resolved sufficiently to allow estimates of the peak volume. When cross peaks are close enough to give rise to concern about possible overlap, a carefully selected portion of each cross peak, as far removed as possible from the vicinity of the other cross peak, was used to obtain the exchange data. A few of the exchange curves show evidence of the contribution of more than one resonance, in the form of a two-exponential decay. For these, a two-exponential least-squares fit to the data was calculated and the exchange rates obtained from the fit were assigned according to a visual estimate of the position of the longer-remaining cross peak. Only for the resonances of Asp 43 and Glu 44 in Trx-$(SH)_2$ and Ile 45 and Glu 48 in Trx-S_2 were such corrections necessary.

Even after several weeks in $^{2}H_2O$, there were persistent amide protons, indicated by the presence of cross peaks in the $^{15}N-^{1}H$ HSQC spectrum, as shown in Figure 2. It is clear that the number of cross peaks is greater for Trx-S_2 (Figure 2A) than for Trx-$(SH)_2$ (Figure 2B), again providing strong evidence of a measurable difference in the hydrogen exchange behavior of the two forms of the protein.

The H−D exchange rate was determined for each amide proton from least-squares fits to the exponential decay of the cross-peak volume as a function of time; examples of such plots are shown in Figure 3. Most of the exchange rates are virtually identical for a given proton in the two forms of the protein, as shown in Figure 3A, but for a number of protons in the vicinity of the active site the rates are different, as shown in Figure 3B. The amide proton exchange rates calculated from the hydrogen−deuterium exchange data are shown in Table 1, together with the intrinsic rate constants calculated using the method of Bai *et al.* (1993) and the protection factors calculated from these values (see below).

Measurement of Exchange Rates by Saturation Transfer. For a number of residues, principally those in turns and loops of the molecule, the exchange rates are too rapid to measure by H−D exchange. For these residues, an estimate of the

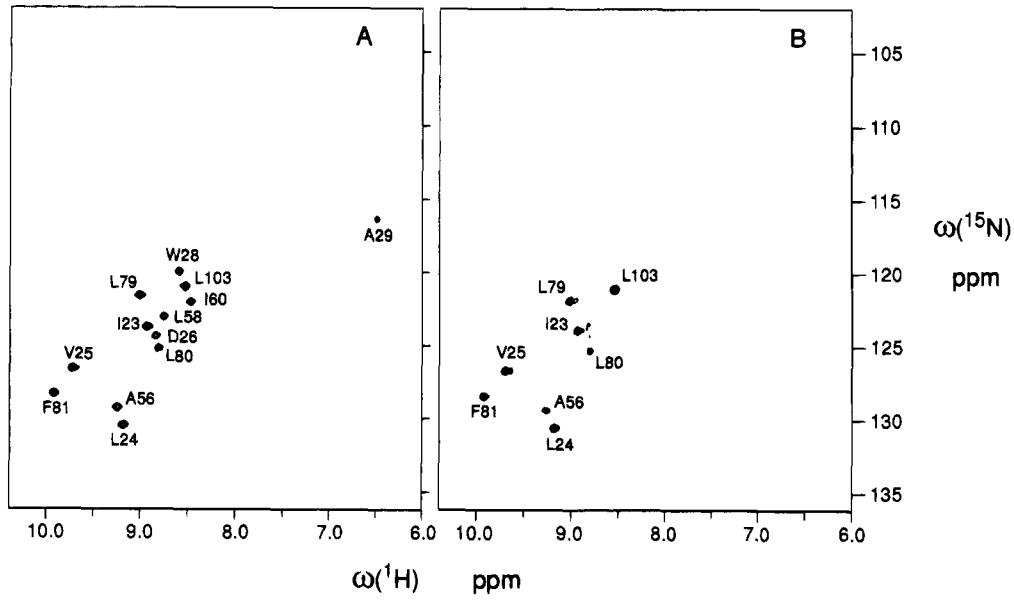

FIGURE 2: $^{15}N-^{1}H$ HSQC spectra of (A) Trx-S_2 and (B) Trx-$(SH)_2$ showing the latest time point (723 and 711 h, respectively, after transfer into $^{2}H_2O$).

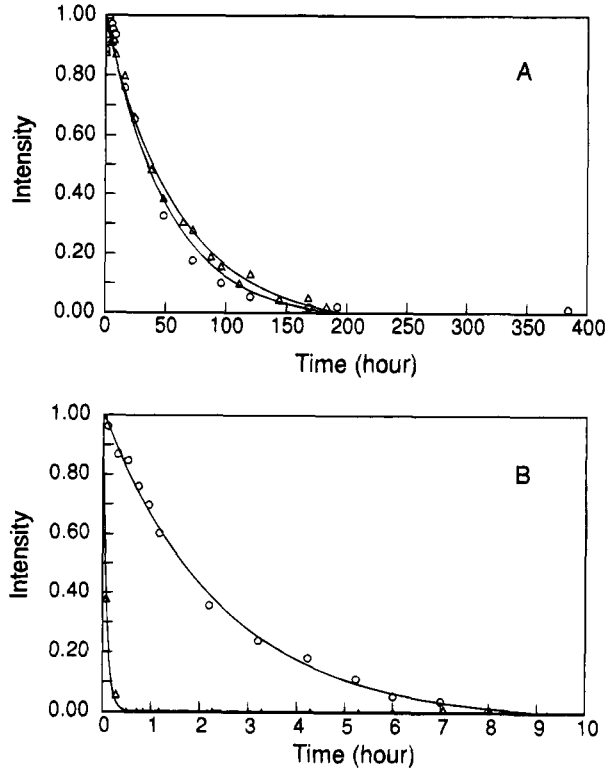

FIGURE 3: Plots showing the time course of decay of $^{15}N-^{1}H$ HSQC cross peak intensity, normalized to give an intensity of 1.0 for the first point. (A) Lys 57 in Trx-S_2 (○) and Trx-$(SH)_2$ (△) (B) Ile 38 in Trx-S_2 (○) and Trx-$(SH)_2$ (△). Solid lines are exponential decays fitted to the data by the method of least squares.

exchange rate was obtained by saturation-transfer measurements (Hoffman & Forsén, 1966). Several factors can introduce error into such estimates. Attenuation of the amide proton resonances by saturation transfer upon irradiation of the residual $^{1}HO^{2}H$ resonance has been observed for resonances within 200 Hz of the point of irradiation (Skelton *et al.*, 1992); the width of the spectrum affected is dependent on the strength of the decoupling field. None of the NH resonances of thioredoxin are affected directly in this way, since the highest-field amide proton resonance (Cys 32 in Trx-$(SH)_2$) is at 6.51 ppm, 1020 Hz from the water resonance at 298 K and 500 MHz. Truncated driven nuclear Overhauser effects can attenuate the cross peaks, if the NH resonances have NOEs to protons resonating between 4.5 and 5 ppm (Skelton *et al.*, 1992), a region that includes many of the $C^{\alpha}H$ resonances. According to the published resonance assignments, 43 of the 101 amide protons in thioredoxin could have sequential or intraresidue NOEs to protons resonating between 4.5 and 5.0 ppm, and 19 of these are among the 32 fast-exchanging amides whose exchange rates are to be measured by saturation transfer. A correction for the effects of the NOE can be made by measuring and calculating the exchange rates at two pH values (Campbell *et al.*, 1978). These measurements have been made for Trx-S_2 and Trx-$(SH)_2$, and the resulting exchange rates appear in Table 1. The two pH values were carefully chosen to minimize the effects of the titration of several ionizable groups in the active site region, including the carboxyl side chain of Asp 26 and the thiol of Cys 32 (Dyson *et al.*, 1991). A total of 33 amide proton exchange rates were estimated in this way for Trx-$(SH)_2$, and 32 for Trx-S_2, this difference reflecting the behavior of the Cys 35 amide, as mentioned previously. The exchange rates for His 6 are given as a lower limit only: the rate is too rapid for quantitation by H−D exchange measurements, and the two pHs used in the saturation-transfer experiments, 5.7 and 6.1, are too close to the pK_a of the His 6 side chain, 5.9 (Dyson *et al.*, 1991), for a reliable measurement to be made by this method. The data obtained from the saturation-transfer experiment are only reliable for quite fast exchange rates, greater than about 0.25 s^{-1} at pH 6.1 (Campbell *et al.*, 1978). Slower rates correspond to a difference of less than approximately 10% in the cross-peak volumes obtained at the two pHs; the uncertainty in the cross-peak volume data make the k_{ex} values obtained from eq 3 unreliable in such cases. The amide protons for which the exchange rate was too slow to measure by saturation transfer for this reason, but which nevertheless exchange too fast to be observed in the H−D experiments, have been assigned an intermediate rate, indicated by a range of exchange rate in Table 1.

The measured exchange rates shown in Table 1 are plotted according to residue number in Figure 4A. The identities

Table 1: Exchange Rates and Protection Factors for Trx-S_2 and Trx-$(SH)_2$

residue	log k_{int}	log k_{ex}[a]		log PF		residue	log k_{int}	log k_{ex}[a]		log PF	
		Trx-S_2	Trx-$(SH)_2$	Trx-S_2	Trx-$(SH)_2$			Trx-S_2	Trx-$(SH)_2$	Trx-S_2	Trx-$(SH)_2$
3 Lys[b]	−0.29	−0.02	−0.02	−0.27	−0.27	56 Ala	−0.60	−8.4[a]	−7.0[a]	7.8	6.4
4 Ile	−1.07	−2.71	−2.81	1.64	1.74	57 Lys	−0.50	−5.60	−5.66	5.10	5.16
5 Ile	−1.42	−4.06	−4.13	2.64	2.71	58 Leu	−0.92	−8.2[a]	−7.5[a]	7.3	6.6
6 His[c]	0.91	−2.6[c]	−2.6[c]	3.5[c]	3.5[c]	59 Asn[b]	0.59	−0.64	−0.20	1.23	0.79
7 Leu	−0.21	−4.00	−4.17	3.79	3.96	60 Ile	−0.87	−6.80	−6.44	5.93	5.57
8 Thr	−0.74	−5.01	−5.02	4.27	4.28	61 Asp	−1.00	−5.12	−4.66	4.12	3.66
9 Asp	−0.56	−3.11	−3.28	2.55	2.72	62 Gln	−0.58	−2.72	−3.10	2.14	2.52
10 Asp[b]	−0.17	−0.21	0.12	0.04	−0.29	63 Asn	0.23	−4.80	−4.62	5.03	4.85
11 Ser	−0.27	−3.09	−3.22	2.82	2.95	65 Gly[b]	0.34	*d*	*d*	2.9−0.9[d]	2.9−0.9[d]
12 Phe	−0.40	−4.18	−4.18	3.78	3.78	66 Thr	−0.36	−4.36	−4.15	4.00	3.79
13 Asp[b]	0.08	*d*	−0.40	2.7−0.7[d]	0.48	67 Ala	−0.26	−4.66	−4.54	4.40	4.28
14 Thr	−0.71	−3.24	−3.31	2.53	2.60	69 Lys	−0.74	−3.21	−3.09	2.47	2.35
15 Asp	−0.56	−3.51	−3.49	2.95	2.93	70 Tyr	−0.61	−5.06	−4.91	4.45	4.30
16 Val	−1.35	−5.40	−5.44	4.05	4.09	71 Gly[b]	0.63	*d*	−0.31	3.2−1.2[d]	0.94
17 Leu	−1.19	−5.93	−5.97	4.74	4.78	72 Ile	−1.02	−3.69	−3.52	2.67	2.50
18 Lys	−0.71	−4.41	−4.43	3.70	3.72	73 Arg[b]	0.16	−0.14	−0.20	0.30	0.36
19 Ala	−0.34	−2.75	−2.80	2.41	2.46	74 Gly[b]	0.80	−0.19	0.23	0.99	0.57
20 Asp[b]	0.01	*d*	−0.19	2.6−0.6[d]	0.20	75 Ile[b]	−0.24	*d*	−0.01	2.4−0.4[d]	−0.23
21 Gly[b]	0.40	−0.21	−0.12	0.61	0.52	77 Thr	0.07	−4.37	−3.82	4.44	3.89
22 Ala[b]	0.48	*d*	−0.34	3.1−1.1[d]	0.82	78 Leu	−0.84	−5.74	−5.67	4.90	4.83
23 Ile	−1.19	−7.7[a]	−7.6[a]	6.5	6.4	79 Leu	−1.25	−7.6[a]	−7.6[a]	6.3	6.3
24 Leu	−1.28	−7.8[a]	−7.8[a]	6.5	6.5	80 Leu	−1.25	−8.0[a]	−8.0[a]	6.8	6.8
25 Val	−1.38	−8.0[a]	−8.0[a]	6.6	6.6	81 Phe	−0.91	−8.5[a]	−7.6[a]	7.6	6.7
26 Asp	0.09	−7.4[a]	−7.0[a]	7.5	7.1	82 Lys	−0.44	−6.10	−6.06	5.66	5.62
27 Phe	−0.10	−5.65	−5.74	5.55	5.64	83 Asn[b]	0.92	−0.26	−0.03	1.18	0.95
28 Trp	−0.82	−7.5[a]	−6.55	6.6	5.73	84 Gly	0.13	−3.87	−3.89	4.00	4.02
29 Ala	−0.57	−6.66	−5.89	6.09	5.32	85 Glu	−0.80	−5.02	−4.85	4.22	4.05
30 Glu[b]	−0.19	−0.31	−0.46	0.12	0.27	86 Val	−1.31	−2.64	−2.57	1.33	1.26
31 Trp[b]	−0.24	−0.55	−0.34	0.31	0.10	87 Ala	−0.60	−4.74	−4.75	4.14	4.15
32 Cys[b]	*e*	0.37	*d*	0.38	3.4−1.4[d]	88 Ala	−0.46	−4.48	−4.48	4.02	4.02
33 Gly[b]	*e*	0.14	>1.16	0.90	<−0.03	89 Thr[b]	0.25	−0.60	−0.24	0.85	0.49
35 Cys[f]	*e*	−5.07	0.40[b]	4.92	0.29	90 Lys	−0.30	−3.77	−3.69	3.47	3.39
36 Lys[b]	*e*	*d*	*d*	3.3−1.3[d]	3.4−1.4[d]	91 Val[b]	−0.27	*d*	*d*	2.3−0.3[d]	2.3−0.3[d]
37 Met[b]	0.42	*d*	*d*	3.0−1.0[d]	3.0−1.0[d]	92 Gly[b]	0.44	*d*	−0.02	3.0−1.0[d]	0.46
38 Ile	−1.09	−4.28	−2.82	3.19	1.73	93 Ala[b]	0.48	−0.59	−0.68	1.07	1.16
39 Ala	−0.69	−3.08	−2.81	2.39	2.12	94 Leu[b]	−0.27	−0.48	−0.11	0.21	−0.16
41 Ile	−1.43	−4.70	−4.27	3.27	2.84	95 Ser[b]	0.47	*d*	*d*	3.1−1.1[d]	3.1−1.1[d]
42 Leu	−1.28	−5.86	−3.64	4.58	2.36	96 Lys[b]	0.58	−0.54	−0.60	1.12	1.18
43 Asp	−0.97	−3.81	−3.80	2.84	2.83	97 Gly[b]	0.71	*d*	−0.08	3.3−1.3[d]	0.79
44 Glu	−1.15	−4.31	−4.35	3.16	3.20	98 Gln[b]	0.54	*d*	−0.25	3.1−1.1[d]	0.79
45 Ile	−1.35	−6.10	−5.98	4.75	4.63	99 Leu	−0.84	−3.74	−3.84	2.90	3.00
46 Ala	−0.69	−5.90	−5.93	5.21	5.24	100 Lys	−0.71	−5.18	−5.14	4.47	4.43
47 Asp	−0.76	−3.73	−3.90	2.97	3.14	101 Glu	−0.85	−5.62	−5.54	4.77	4.69
48 Glu	−1.12	−4.31	−4.36	3.19	3.24	102 Phe	−0.85	−4.26	−4.28	3.41	3.43
49 Tyr	−0.88	−4.04	−4.03	3.16	3.15	103 Leu	−0.98	−7.51	−7.47	6.53	6.49
50 Gln	−0.35	−2.85	−2.86	2.50	2.51	104 Asp	−0.97	−6.47	−6.41	5.50	5.44
51 Gly[b]	0.78	0.13	0.28	0.65	0.50	105 Ala	−0.64	−3.94	−3.80	3.30	3.16
52 Lys[b]	0.44	−0.51	−0.19	0.95	0.63	106 Asn	0.03	−4.21	−4.29	4.24	4.32
53 Leu	−0.92	−4.62	−4.23	3.70	3.31	107 Leu	−0.72	−3.55	−3.35	2.83	2.63
54 Thr	−0.74	−6.54	−6.37	5.80	5.63	108 Ala[b]	−1.70	*d*	*d*	0.9 to −1.1[d]	0.9 to −1.1[d]
55 Val	−0.96	−5.10	−5.09	4.14	4.13						

[a] An estimate of the error for the H−D exchange data was obtained from the least-squares fits. Error estimates obtained in this way were generally about 5%, except for the slowest exchanging amides. Where cross-peak intensity was diminished by less than 10% at the longest time point, the error estimate was higher, and the rates and protection factors are therefore quoted to only two significant figures. [b] Exchange rates too rapid for measurement by H−D exchange were measured by saturation transfer in ^1H_2O. These exchange rates are quoted at pH 6.1 and are directly comparable to the H−D exchange rates at pH(apparent) 5.7, due to the deuterium isotope effect. [c] Exchange rates for His 6 are given as a lower limit only (see text). [d] Exchange rates for these amide protons were intermediate between the ranges accessible for measurement by saturation transfer (0.25−25 s^{-1}) and H−D exchange (≤0.0025 s^{-1}). Therefore the intermediate exchange rates are in the range 0.0025−0.25 s^{-1} (log value −2.6 to −0.6) at pH 6.1, and the corresponding protection factors are also shown as a range. [e] Intrinsic exchange rates for Cys 32 are 0.75 (Trx-S_2) and 0.82 (Trx-$(SH)_2$), for Gly 33 are 1.04 (Trx-S_2) and 1.13 (Trx-$(SH)_2$), for Cys 35 are −0.15 (Trx-S_2) and 0.69 (Trx-$(SH)_2$), and for Lys 36 are 0.73 (Trx-S_2) and 0.82 (Trx-$(SH)_2$). [f] The exchange rate was measured by H−D exchange for Trx-S_2, but the rate for Trx-$(SH)_2$ was too rapid for measurement by this means and was instead measured by saturation transfer.

of "slowly exchanging" amide protons in the two forms of thioredoxin have been published previously (Dyson *et al.*, 1989). All of the present results are consistent with the previous observations; the rate threshold above which the protons were not observed in the previous work appears to be ~10^{-5} s^{-1} from the figure, and the majority of the slowly exchanging amide protons identified (70%) were in the β-sheets. In contrast, the H−D exchange measurements in the present work, which utilize rapidly acquired HSQC NMR spectra, are able to detect and measure amide proton exchange rates as fast as 2.5 × 10^{-3} s^{-1}, and the amide protons in the four helices of the molecule are much better represented.

Calculation of Protection Factors. In order to determine the structural contribution to hydrogen exchange, protection factors were calculated (Jeng *et al.*, 1990). The protection

factor is given by

$$P = k_{int}/k_{ex}$$

where k_{ex} is the measured exchange rate and k_{int} is the intrinsic exchange rate for each residue. The intrinsic exchange rates were calculated from free peptide exchange rates (Jeng & Englander, 1991; Englander & Poulsen, 1969; Englander *et al.*, 1979), corrected for the effects of local sequence differences (Molday *et al.*, 1972; Bai *et al.*, 1993) and calibrated for the pH and temperature of the exchange experiments (Jeng & Englander, 1991; Englander & Poulsen, 1969). The results are listed in Table 1 and shown plotted according to residue number in Figure 4B. The activation energies used for calculation of hydrogen exchange rates at the temperature of the experiment, 298 K, are 14, 17, and 19 kcal mol^{-1} for acid, base, and water catalysis, respectively (Bai *et al.*, 1993). As expected, the intrinsic exchange rates vary quite widely between residues of the same type, depending on the nature of the preceding residue. A particularly noticeable case concerns Asp 26, which has an intrinsic exchange rate much larger than those of other Asp residues in the protein. This is because we have assumed that the side chain of this residue is protonated at the pH of the experiment (5.7), consistent with the shifted Asp 26 pK_a ~ 7.0 previously obtained for Trx-S_2 and Trx-$(SH)_2$ (Dyson *et al.*, 1991). Other aspartates have been assumed to be deprotonated at pH 5.7, consistent with a more normal pK_a of ~4.0.

Correlation of Protection Factors with the Structure of Thioredoxin. The total number of amide protons for which hydrogen exchange data have been measured is 101, corresponding to all of the residues in thioredoxin except the five prolines and the N-terminal residues Ser 1 and Asp 2. The amide proton of Asp 2 has never been observed in either form of thioredoxin, presumably due to extremely fast exchange with solvent. In general, the residues for which the amide proton exchange rates are measurable by H−D exchange are present in hydrogen-bonded secondary structure, while the amide protons that exchange rapidly and are therefore investigated by saturation transfer are in turn and loop sequences between the elements of secondary structure, with the exception of residues 89 and 91, which form part of the fifth β-strand of the central β-sheet, and His 6, which is in the middle of the first β-strand. The structure of thioredoxin (Jeng *et al.*, 1994) indicates that the amide protons of His 6, Thr 89, and Val 91 extend toward the outside of the sheet and are therefore not hydrogen-bonded, so the faster exchange rates of these residues are not unexpected. The presence of hydrophilic side chains and glycine residues in the vicinity are probably also contributing factors to the faster exchange of these amide protons. Neighboring residues such as Ile 5, Leu 7, Ala 88, and Lys 90, whose amide protons extend toward the β-sheet, have slower exchange rates, due to hydrogen bonding and protection in the hydrophobic core of the molecule. The general pattern of the rapidly exchanging amide protons is therefore consistent with the structure of thioredoxin.

It is noticeable from Table 1 that all of the glycine residues in the molecule, with the exception of Gly 84, have amide protons that exchange too rapidly to be measured by H−D exchange. This is consistent with the small size of glycine and with its preference for flexible loop and turn regions of the protein. A number of the glycine residues show a small

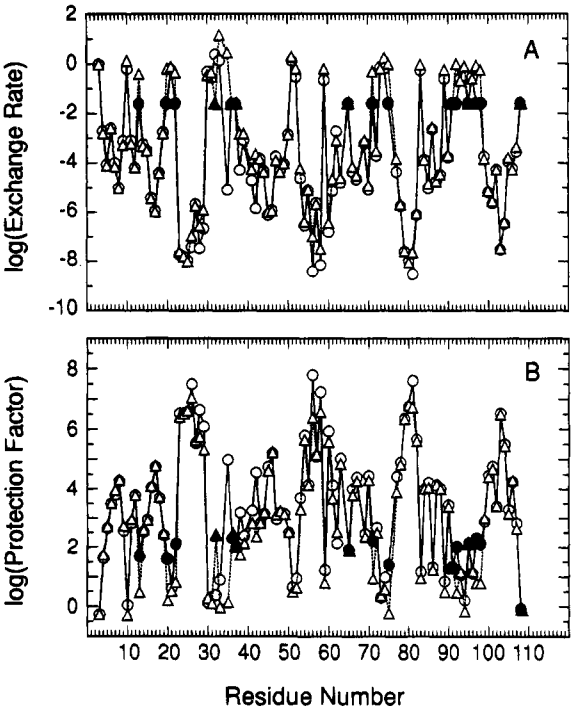

FIGURE 4: Logarithm of (A) exchange rate and (B) protection factor, plotted as a function of residue number. Open circles connected by solid lines represent data for Trx-S_2, and open triangles connected by dotted lines represent data for Trx-$(SH)_2$. Solid circles and triangles show the centers of the ranges of exchange rate and protection factor for those residues that have intermediate exchange rates not well-determined by either saturation-transfer or hydrogen−deuterium exchange methods.

difference in the exchange behavior in saturation transfer experiments between Trx-S_2 and Trx-$(SH)_2$ (Table 1). While the uncertainties in these measurements are in general considerably greater than those for the H−D exchange measurements, due to the necessity for obtaining the exchange rates from the subtraction of two peak volumes from different NMR spectra (eq 3), it is clear that there is a significant qualitative difference between the exchange rates for a number of residues in turns and loops, indicated by the rate being fast enough to measure in Trx-$(SH)_2$ and in the intermediate exchange region in Trx-S_2. These residues include glycines 71, 92, and 97; aspartates 13 and 20; Ala 22; Ile 75; and Gln 98. Thus, a general trend is seen among the fastest-exchanging amide protons, present in the turns and loops of the molecule and therefore exposed to solvent, for the exchange to be slightly but significantly faster for Trx-$(SH)_2$.

The amide protons of several residues show extremely slow exchange rates. These include Ile 23, Leu 24, Val 25, Asp 26, Ala 56, Leu 58, Leu 79, Leu 80, and Phe 81. Residues 23−26 are present in the central strand of the β-sheet (Dyson *et al.*, 1989). The amide protons of residues 56 and 58, in the second β-strand, and residues 81 and 79, in the fourth β-strand, extend toward this central strand. Thus, with the exception of Leu 80, the amide protons that show extremely slow rates of exchange are associated directly with the central strand of the sheet and would thus be most likely to be strongly hydrogen-bonded and well-protected in the hydrophobic core of the molecule. A small but significant difference in the exchange rates of several of these amide protons is observed between Trx-$(SH)_2$ and Trx-S_2. This is illustrated in Figure 2, where cross peaks are observed in the longest-time ^{15}N HSQC spectrum of Trx-S_2 that are

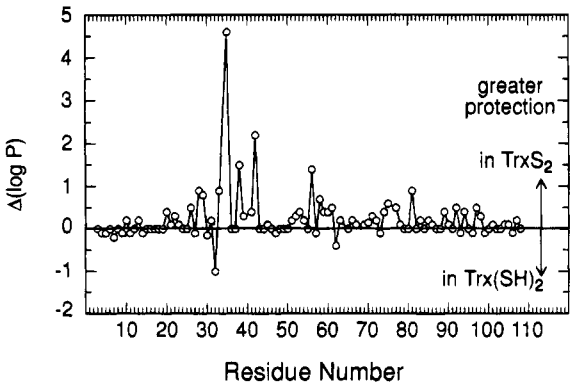

FIGURE 5: Difference in (log protection factor) ΔP (= log P(Trx-S_2) − log P(Trx-$(SH)_2$) between residues in Trx-S_2 and Trx-$(SH)_2$. Where an intermediate exchange rate is involved (two values in Figure 4B) the difference is taken to the closer of the two values defining the range, thus giving the lower limit of the difference ΔP.

absent from that of Trx-$(SH)_2$. The residues for which these differences are observed are present in the β-sheet in the region closest to the active site, Asp 26, Trp, 28 and Leu 58. The structures of the two forms of thioredoxin determined by NMR (Jeng *et al.*, 1994) show no significant difference in backbone or side-chain conformation for these residues; the hydrogen exchange measurements indicate, however, that the structure of Trx-$(SH)_2$ is, in some small but significant way, more flexible in this region, allowing greater access of solvent for hydrogen exchange in the core of the molecule.

Several residues in the three major helices show significant slowing of amide proton exchange. Such slowing is periodic; the residues involved are present in the packing interfaces between the helices and the remainder of the molecule, and several of the side chains are part of the hydrophobic core. For example, Val 16, for which the resonances of the methyl groups are shifted to high field due to its interaction with several aromatic rings, has an exchange rate of 4×10^{-4} s^{-1} (Table 1), and Leu 103 shows no sign of a reduction in HSQC peak volume even after several weeks (Figure 2).

Hydrogen Exchange in Oxidized and Reduced Thioredoxin. As illustrated in Figure 5, a number of residues close to the active site have significantly different amide proton exchange rates in the two forms of thioredoxin. Within the active site and in a number of adjacent loops the amide proton exchange rates are generally rapid, consistent with the generally lower values of the order parameter S^2 obtained from ^{15}N relaxation measurements for these regions, reflecting increased local mobility (Stone *et al.*, 1993). Several of these residues, for example Gly 33, Ile 75, and Gly 92, show small but significant increases in exchange rates, measured by saturation transfer, for Trx-$(SH)_2$ (Table 1). Significant increases are observed in the active site itself and in the secondary structure in the vicinity of the active site.

The most significant difference in exchange rates between Trx-S_2 and Trx-$(SH)_2$ occurs for the amide proton of Cys 35. The rate obtained from the H−D exchange measurements for this residue in Trx-S_2 is 8.5×10^{-6} s^{-1}, while that obtained from saturation-transfer measurements for Trx-$(SH)_2$ is 2.5 s^{-1}, a difference of more than 5 orders of magnitude. There are doubtless a number of factors that contribute to so large a difference in rate, including the different properties of the cysteine and half-cystine side chains. According to the solution structures of Trx-S_2 and Trx-$(SH)_2$ (Jeng *et al.*, 1994) the position of the Cys 35 backbone and side chain is the same in the two molecules, and the solvent exposure of the Cys 35 amide group is zero for both. However, a significant difference in the hydrogen bonding of the Cys 35 amide proton was found: in Trx-S_2 the Cys 35 NH is hydrogen bonded to two acceptors, the Cys 32 CO and the Cys 32 S. In Trx-$(SH)_2$ the only possible hydrogen-bonding partner is the Cys 32 CO, as the side chain of Cys 32 has swung out into the solvent to accommodate the van der Waals radii of the two sulfur atoms (Jeng *et al.*, 1994).

An apparent faster exchange rate is seen in Trx-S_2 for only one residue, Cys 32 (Table 1). There is no obvious explanation from the solution structures for such a difference (Jeng *et al.*, 1994). It should also be noted that since the upper limit of the range of intermediate rates approaches within an order of magnitude the rate observed for Trx-S_2, the actual difference in exchange rates for this residue between the two forms may not be highly significant. There is also a question as to the validity of the measurement for Cys 32 in particular, first because of the proximity of the $C^{\alpha}H$ resonances of both Cys 32 and the preceding residue, Trp 31, to that of H_2O (Dyson *et al.*, 1989), together with the slight differences in backbone NOE intensities and conformation between Trx-S_2 and Trx-$(SH)_2$ that occur in this region (Jeng *et al.*, 1994), and finally because of the pK_a of the Cys 32 thiol group in Trx-$(SH)_2$. Deprotonation of the Cys 32 thiol occurs with a low pK_a, which has been evaluated by various means to be between 6.7 and 7.0 (Kallis & Holmgren, 1980; Dyson *et al.*, 1991). The estimation of the exchange rates in the saturation-transfer experiments relies upon the difference between spectra acquired at two different pHs (Campbell *et al.*, 1978); the pHs for the thioredoxin measurements, 5.7 and 6.1, were chosen to minimize the effects of the Cys 32 titration. It is possible that the Trx-$(SH)_2$ Cys 32 amide proton nevertheless feels an effect of the beginning of the titration and that the results at the higher pH, closer to the pK_a, do not reflect the behavior of the same state of the molecule as at pH 5.7, and therefore that the rate estimates are biased for the reduced form of the protein. Thus, while we note that a lower rate for the Cys 32 amide proton exchange in Trx-$(SH)_2$ is apparent, we do not offer exhaustive discussion on this point, as the results are somewhat equivocal.

Local Unfolding Indicated by Hydrogen Exchange. Under the conditions of the NMR experiments it is clear that local unfolding of the EX_2 type rather than global unfolding of the EX_1 type (Hvidt & Nielsen, 1966) is more likely to be the mechanism by which hydrogen exchange occurs in thioredoxin. If this is the case, it is possible to identify groups exposed by the same local opening motion of the protein by observing points that lie on straight lines of unit slope in plots of log k_{ex} against log k_{int} (Wagner, 1983). This is illustrated in Figure 6 for the helix $\alpha 2$ following the active site. The behavior of this helix is complicated by the presence of Pro 40 in the middle of the helix and by the active site at the N-terminal end. Three sets of amide protons can be identified from this graph, with residues at the C-terminal end of the helix (residues 47−50) in one group and residues in the middle (45 and 46) in another, indicating that the helix is fraying in a standard pattern at the C-terminal end. At the N-terminal end, residues 35−42 appear along one line for Trx-$(SH)_2$, indicating that they are exposed by the same opening motion and that N-terminal fraying is

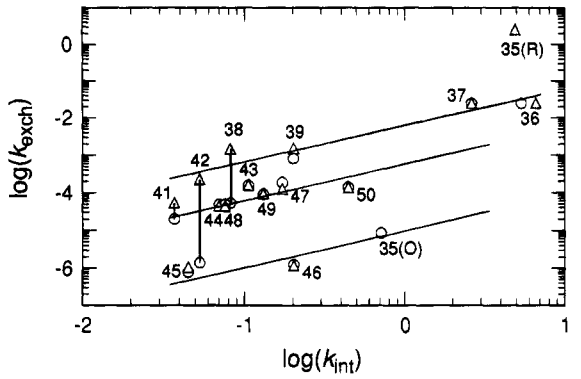

FIGURE 6: Plot of the logarithm of the intrinsic exchange rate (k_{int}) against the logarithm of the measured exchange rate (k_{exch}) for the helix α2 following the active site (residues 35−50, labeled accordingly). Circles indicate data for Trx-S_2, and triangles, that for Trx-$(SH)_2$. The oblique lines with unit slope are drawn to indicate the three groups of amide protons mentioned in the text.

extensive and includes residues beyond Pro 40. By contrast, N-terminal fraying in Trx-S_2 appears to be limited to residues 36 and 37; Leu 42 is now part of the set that includes the central residues Ile 45 and Ala 46. A similar plot (not shown) for residues in the β-sheet indicates that the local unfolding of the sheet probably occurs, as expected, first from the edge strands and from the ends of each strand. The β-sheet amide protons with exchange rates lower in Trx-S_2 than in Trx-$(SH)_2$ either point toward the α2 helix (Ala 56, Leu 58, Asp 26, Phe 81) or are close to the active site disulfide (Trp 28, Ala 29). This differential effect is also apparently due to the N-terminal fraying of the α2 helix in Trx-$(SH)_2$.

Implications for Solution Structure and Function of Thioredoxin. Only the most subtle changes are seen in the active site structure upon reduction of Trx-S_2, involving mainly small changes in backbone structure of residues 31 and 32 to accommodate the van der Waals radii of the two thiols (Jeng *et al.*, 1994). Nevertheless, the two forms of thioredoxin show greatly different reactivity in certain bacteriophage systems, including T7 DNA polymerase and filamentous phage assembly, where Trx-$(SH)_2$ is functional but Trx-S_2 is not (Adler & Modrich, 1983; Russel & Model, 1985). The major determining factor in this difference does not appear to be the presence of free thiol groups, since mutants of thioredoxin where one or both cysteines are replaced by alanine or serine are also partly functional (Russel & Model, 1986; Adler & Modrich, 1983). Differences between Trx-$(SH)_2$ and Trx-S_2 that are less structural than dynamic have been postulated to explain these differences in behavior (Stone *et al.*, 1993; Jeng *et al.*, 1994). The hydrogen exchange results for thioredoxin clearly demonstrate that the backbone of Trx-$(SH)_2$ is significantly more flexible than that of Trx-S_2 in the vicinity of the active site, not only in the immediate vicinity of the active site disulfide itself but also propagated along the highly ordered secondary structure elements adjacent to the active site in the sequence of the protein. We see significant differences in the exchange rates of Asp 26, in the preceding β-strand, and of Leu 42, in the following helix, with the implication that the entire region of the active site is more accessible to solvent in the reduced form of the protein, possibly due to a concerted fraying of the N-terminal half of the helix.

While the most significant differences in the hydrogen exchange rates of amide protons in Trx-S_2 and Trx-$(SH)_2$ are in the local region surrounding the active site, a small but consistent increase in exchange rate is observed for Trx-$(SH)_2$ amide protons even quite distant from the active site. In particular, the rates observed for the residues in the center of the β-sheet are consistently higher for Trx-$(SH)_2$. This raises questions that are relevant to a number of previous studies. The thermal stability of thioredoxin in both oxidation states is high (Hiraoki *et al.*, 1988). However, there is a significant difference in the midpoint of the thermal denaturation curve for the two forms: the midpoint is some 10 °C higher for Trx-S_2. Since the only difference between the two forms of the protein is a single disulfide bond between residues separated by only two amino acids in the sequence, and since the structures of the two forms are very similar (Jeng *et al.*, 1994), the difference in melting temperature seems high. Differences have also been observed in the partial specific volume and adiabatic compressibility of the two forms of thioredoxin (Kaminsky & Richards, 1992b) also appear inconsistent with the very subtle structural changes observed. It was suggested that alterations in the solvation of the entire molecule upon change of oxidation state could be responsible for the observed changes in thermodynamic properties (Kaminsky & Richards, 1992b). Both the backbone dynamics measurements (Stone *et al.*, 1993) and the hydrogen exchange measurements (this work) demonstrate a significant difference in the flexibility of the active site region between the two oxidation states. The hydrogen exchange measurements hint that the effect may be more widespread in the molecule than is indicated by a simple examination of S^2 values. We suggest that the two hypotheses, change of mobility and change of solvation, are not incompatible and may be used together to explain many of the functions and physical properties of thioredoxin.

ACKNOWLEDGMENT

We thank Martin Stone, V. V. Krishnan, and Peter Wright for helpful discussions and Linda Tennant for expert technical assistance. The ^{15}N-labeled protein was kindly provided by Arne Holmgren.

REFERENCES

Adler, S., & Modrich, P. (1983) *J. Biol. Chem. 258*, 6956−6962.

Bai, Y., Milne, J. S., Mayne, L., & Englander, S. W. (1993) *Proteins 17*, 75−86.

Bax, A., Ikura, M., Kay, L. E., Torchia, D. A., & Tschudin, R. (1990) *J. Magn. Reson. 86*, 304−318.

Campbell, I. D., Dobson, C. M., Ratcliffe, R. G., & Williams, R. J. P. (1978) *J. Magn. Reson. 29*, 397−417.

Chandrasekhar, K., Krause, G., Holmgren, A., & Dyson, H. J. (1991) *FEBS Lett. 284*, 178−183.

Chandrasekhar, K., Campbell, A. P., Jeng, M.-F., Holmgren, A., & Dyson, H. J. (1994) *J. Biomol. NMR 4*, 411−432.

Connelly, G. P., Bai, Y., Jeng, M.-F., & Englander, S. W. (1993) *Proteins 17*, 87−92.

Dyson, H. J., Holmgren, A., & Wright, P. E. (1989) *Biochemistry 28*, 7074−7087.

Dyson, H. J., Gippert, G. P., Case, D. A., Holmgren, A., & Wright, P. E. (1990) *Biochemistry 29*, 4129−4136.

Dyson, H. J., Tennant, L. L., & Holmgren, A. (1991) *Biochemistry 30*, 4262−4268.

Englander, S. W., & Poulsen, A. (1969) *Biopolymers 7*, 379−393.

Englander, J. J., Calhoun, D. B., & Englander, S. W. (1979) *Anal. Biochem. 92*, 517−524.

Forsén, S., & Hoffman, R. A. (1963) *J. Chem. Phys. 39*, 2892.
Hiraoki, T., Brown, S. B., Stevenson, K. J., & Vogel, H. J. (1988) *Biochemistry 27*, 5000−5008.
Hoffman, R. A., & Forsén, S. (1966) *Prog. NMR Spectrosc. 1*, 15−204.
Holmgren, A. (1985) *Annu. Rev. Biochem. 54*, 237−271.
Huber, H. E., Russel, M., Model, P., & Richardson, C. C. (1986) *J. Biol. Chem. 261*, 15006−15012.
Hughson, F. M., Wright, P. E., & Baldwin, R. L. (1990) *Science 249*, 1544−1548.
Hvidt, A., & Nielsen, S. O. (1966) *Adv. Protein Chem. 21*, 287−339.
Jeng, M.-F., & Englander, S. W. (1991) *J. Mol. Biol. 221*, 1045−1061.
Jeng, M.-F., Englander, S. W., Elöve, G. A., Wand, A. J., & Roder, H. (1990) *Biochemistry 29*, 10433−10437.
Jeng, M.-F., Campbell, A. P., Begley, T., Holmgren, A., Case, D. A., Wright, P. E., & Dyson, H. J. (1994) *Structure 2*, 853−868.
Kallis, G. B., & Holmgren, A. (1980) *J. Biol. Chem. 255*, 10261−10265.
Kaminsky, S. M., & Richards, F. M. (1992a) *Protein Sci. 1*, 10−21.
Kaminsky, S. M., & Richards, F. M. (1992b) *Protein Sci. 1*, 22−30.
Katti, S. K., LeMaster, D. M., & Eklund, H. (1990) *J. Mol. Biol. 212*, 167−184.
Messerle, B. A., Wider, G., Otting, G., Weber, C., & Wüthrich, K. (1989) *J. Magn. Reson. 85*, 608−613.
Molday, R. S., Englander, S. W., & Kallen, R. G. (1972) *Biochemistry 11*, 150−158.
Norwood, T. J., Boyd, J., Heritage, J. E., Soffe, N., & Campbell, I. D. (1990) *J. Magn. Reson. 87*, 488−501.
Roder, H. (1989) *Methods Enzymol. 176*, 446−473.
Russel, M., & Model, P. (1985) *Proc. Natl. Acad. Sci. U.S.A. 82*, 29−33.
Russel, M., & Model, P. (1986) *J. Biol. Chem. 261*, 14997−15005.
Skelton, N. J., Kördel, J., Akke, M., & Chazin, W. J. (1992) *J. Mol. Biol. 227*, 1100−1117.
Spera, S., Ikura, M., & Bax, A. (1991) *J. Biomol. NMR 1*, 155−165.
Stone, M. J., Chandrasekhar, K., Holmgren, A., Wright, P. E., & Dyson, H. J. (1993) *Biochemistry 32*, 426−435.
van de Ven, F. J. M., Janssen, H. G. J. M., Gräslund, A., & Hilbers, C. W. (1988) *J. Magn. Reson. 79*, 221−235.
Wagner, G. (1983) *Q. Rev. Biophys. 16*, 1−57.

BI942065I